Received: 12 August 2016 | Revised: 22 December 2016 | Accepted: 5 January 2017

DOI 10.1002/poc.3685

WILEY Journal of Physical Organic Chemistry

RESEARCH ARTICLE

Comparative charge transfer studies in nonmetallated and metallated porphyrin fullerene dyads

Neha Gupta[1] | Samya Naqvi[1] | Mukesh Jewariya[1,2,3] | Suresh Chand[1] | Rachana Kumar[1]

[1] CSIR-National Institute of Solar Energy, Organic and Hybrid Solar Cells Group, Physics of Energy Harvesting Division, CSIR-National Physical Laboratory, New Delhi, India

[2] Center for Quantum-Beam-based Radiation Research, Korea Atomic Energy Research Institute (KAERI), South Korea

[3] Ultrafast Optoelectronics and Terahertz Photonics Lab, Physics of Energy Harvesting Division, National Physical Laboratory, New Delhi, India

Correspondence
Rachana Kumar, Organic and Hybrid Solar Cells Group, Physics of Energy Harvesting Division, National Physical Laboratory, New Delhi-110012 India.
Email: rachanak.npl@gov.in; rachanak@nplindia.org

Abstract

Single material organic solar cells become an interesting area of research to overcome the challenges with efficient charge separation efficiencies in conventional organic solar cells. In this article, we have synthesized nonmetallated and metallated porphyrin-fullerene dyad materials (H2P-C60 and ZnP-C60, respectively) with simple structure, comprehensively studied their charge transfer mechanism, and established a proof of concept that nonmetallated porphyrin-fullerene dyads are better candidates to be used in organic solar cells compared with metallated dyads. Absorption and electrochemical analysis revealed the ground state electronic interactions between donor-acceptor moieties in both types of dyads. Driving force ($-\Delta G^{o}_{ET}$) for intramolecular electron transfer process was calculated by first oxidation and reduction potentials of dyads. The excited state electronic interactions were characterized by time-resolved fluorescence and pump-probe transient absorption experiments. Strong fluorescence quenching of porphyrin along with reduced lifetimes in dyads due to deactivation of singlet excited states by photoinduced charge transfer process between porphyrin/Zn-porphyrin core and fullerene in different polarity solvents was observed. Transient absorption spectroscopy was also applied to identify the transient spectral features, ie, cationic ($H2P^{+}$/ZnP^{+}) and anionic (C_{60}^{-}) radicals formed because of the charge separation in both types of dyads. Finally, organic solar cell device was also fabricated using the dyads. We obtained higher V_{oc}, J_{sc}, and fill factor in single material organic solar cell using H2P-C60 compared to previous reports.

KEYWORDS

charge transfer, fullerene, porphyrin dyads, solar cells

1 | INTRODUCTION

Table S1. Absorption maxima (λ_{max}, nm) and absorption coefficient (ε, M^{-1} cm^{-1}) of H2P, H2P-C60, and ZnP-C60 in different polarity solvents

Study of photoinduced electron transfer processes in covalently linked fullerene-porphyrin-based donor-acceptor dyad single materials is one of the potential areas of research owing to their future applications in artificial photosynthesis and organic photovoltaics.[1–4] In conventional organic solar cells (OSCs), absorbed photon generates excitons that are dissociated into free charge carriers at the heterojunction formed by electron donor and acceptor materials interface. The diffusion length of these excitons in organic semiconductors ranges between 10 and 20 nm, and therefore, exciton diffusion to interface and its dissociation into free carriers are the main challenges in OSCs.[5] Electron-hole recombination before reaching the interface due to short exciton diffusion length is one of the main limiting factors for low-organic solar cell efficiency than the theoretically calculated efficiency.[6] Bulk heterojunction (BHJ) solar cell structure is the most promising geometry for OSCs forming electron donor-acceptor interface within the exciton diffusion length,

Neha Gupta, Samya Naqvi, and Rachana Kumar are also at the Academy of Scientific and Innovative Research, New Delhi.

but still, the realization of solution-processed BHJ solar cells possess several unsolved problems, like critical optimization of donor-acceptor material ratio, layer thickness, and fabrication condition, and above all is to obtain ideal nanoscale morphology of active layer. Thermodynamic stability of donor-acceptor phases in active layer is very low and form clusters with time, reducing the overall stability of the device. As a solution to all these problems, single material OSCs (SMOSCs), like covalently linked porphyrin-fullerene donor-acceptor dyads, have been developed showing efficient light harvesting, exciton dissociation, and charge transport.[7–11] Such dyad materials have also found several other applications like photoinduced hydrogen evolution,[12] sensing,[13] catalysis,[14] photodynamic therapy,[15] etc.

Porphyrin and metalloporphyrin represent the efficient light harvesting molecules and offer promising potential in artificial solar energy capture.[16–18] On the other hand, fullerene molecules with spherical structure are known to generate long-lived charge separated states.[19–24] Exploiting the properties of these 2 materials, we found that several dyad systems have been theoretically designed[25,26] and synthesized. The main emphasis was to study the effect of donor-acceptor spacers and the type of attachment on fullerene ball on the process of charge separation and charge recombination.[27,28]

Linker between porphyrin donor and fullerene acceptor in dyads plays an important role and shows profound influence on the rate of photoinduced electron transfer.[29–32] Several types of conjugate linkers, like oligomers and π-extended spacers, have been used and studied for their effect on charge transfer.[33–38] In this present article, we have discussed in detail about ground state interactions via electrochemical analysis and ground state absorption spectroscopy of 2 porphyrin-fullerene dyads (metallated [ZnP-C60] and nonmetallated [H2P-C60], respectively), where porphyrin donor is linked to fullerene acceptor by cyclopropane ring through an aliphatic spacer as shown in Scheme 1.

We have also focused on the charge separation and recombination behaviour of these metallated and nonmetallated porphyrin-linked fullerene dyads and established that nonmetallated porphyrin-fullerene dyads are better for porphyrin-fullerene-based SMOSCs because of their faster charge separation and slower recombination compared with metallated porphyrin-fullerene dyad and showed in OSCs device. As the distribution of electronic charges is directly influenced by the surrounding environment,[39] we have also studied the molecular level charge transfer processes in the presence of different polarity solvents for porphyrin and dyads via time-resolved fluorescence measurements. Photophysics of charge-separated states is compared by steady-state fluorescence and transient absorption (TA) spectroscopy. Finally, solar cell device has been fabricated using dyad material in active layer, and approximately 0.01% efficiency has been obtained with H2P-C60 compared with no light effect in ZnP-C60.

2 | EXPERIMENTAL SECTION

2.1 | Synthesis of A3B porphyrin, 5-(4′-hydroxyphenyl)-10,15,20-triphenylporphyrin (H2P) (Scheme 1)

4-Hydroxy benzaldehyde (6.245mM) was added in a 50-mL propionic acid and dissolved completely. Benzaldehyde

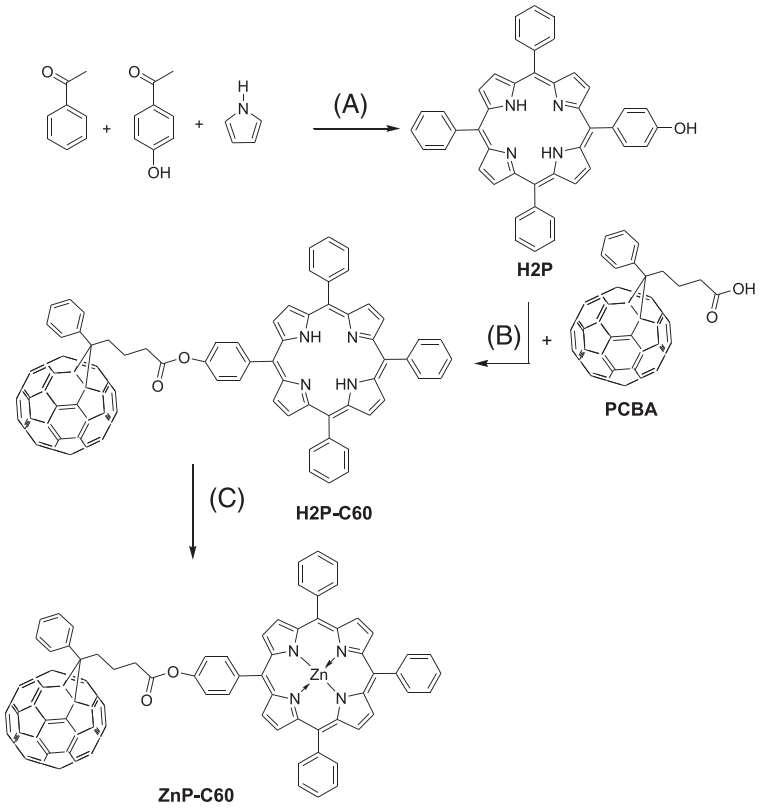

SCHEME 1 Synthesis scheme of porphyrin H2P, dyad H2P-C60, and ZnP-C60. A, Propionic acid, reflux, 30 minutes; B, 4-dimethylaminopyridine, N,N′-dicyclohexylcarbodiimide, 0°C to r.t., 24 hours; C, $Zn(OCOCH_3)_2.2H_2O$, 60°C, 18 hours

(18.735mM) and freshly distilled pyrrole (24.98mM) were added drop wise, and reaction mixture was refluxed with stirring for 30 minutes. Reaction mixture was cooled to room temperature (r.t.) and precipitated with sodium bicarbonate solution. Crude product was collected by filtration and washed several times with methanol followed by purification by column chromatography on silica gel using dichloromethane as eluent. Two fractions were collected. The first one was tetraphenyporphyrin, and the second fraction was the desired product. Evaporation of solvent of fraction 2 left violet crystals that were further recrystallized with dichloromethane yielding violet crystals of porphyrin 1 (H2P). Yield: 12%. Fourier transform infrared spectroscopy (FTIR) (ν, cm^{-1}): 3518, 3321, 2958, 2921, 2851, 1581, 1468, 1258, 1016, 794, 964, and 697; ^1H NMR (400 MHz, $CDCl_3$, δ) (ppm): −2.8 (2H), 7.9 (9H), 8.0 (2H), 8.15 (8H), and 8.76 (8H); ultraviolet-visible (UV-vis) ($CHCl_3$, nm): 412, 515, 550, 591, and 650; HR-MS (MALDI-TOF): m/z[M + 1] for $C_{44}H_{30}N_4O$, calculated 630.2520; found 631.2540.

2.2 | Synthesis of phenyl-C61-butyric acid (PCBA)

For the 50 mg of PCBA methyl ester (PC61BM), 10 mL of toluene was added and stirred well to dissolve. Ten-mililiter glacial acetic acid and 3-mL conc. HCl were added. The reaction mixture was stirred and refluxed for 36 hours. Phenyl-C61-butyric acid being insoluble comes out of reaction mixture and collected by centrifugation. Crude solid is washed several times with toluene to remove minor impurities of unhydrolyzed PC61BM. Dark brown solid is dried at 120°C. Yield: 100%; FTIR (ν, cm^{-1}): 3429, 2921, 2850, 1702, and 1124.

2.3 | Synthesis of H2P-C60 dyad (Scheme 1)

Phenyl-C61-butyric acid (0.0477mM) was sonicated in a mixture 15-mL o-Dichlorobenzene and 5-mL CS_2 for 1 hour followed by addition of H2P (0.0477mM) and further sonicated for an additional 30 minutes to completely dissolve all the components. Reaction mixture was cooled to 0°C, and N,N′-dicyclohexylcarbodiimide (0.3816mM) and 4-dimethylaminopyridine (0.3816mM) were added. Temperature of reaction mixture was raised to r.t. and stirred at this temperature overnight. Solvents were removed on rotary-evaporator, and product (H2P-C60) was isolated by column chromatography (on silica gel with toluene as eluent). Yield: 75%; FTIR (ν, cm^{-1}): 3314, 3057, 1748, 1259, 1163, 1124, 965, 797, and 525; ^1H NMR (400 MHz, $CDCl_3$, δ) (ppm): −2.87 (2H), 2.51 (2H), 2.89 (2H), 3.06 (2H), 7.4 (3H), 7.5 (2H), 7.7 (9H), 7.9 (2H), 8.1 (8H), and 8.77 (8H); UV-vis ($CHCl_3$, nm): 328, 418, 508, 549, 590, and 650; HR-MS (MALDI-TOF): m/z[M-1] for $C_{115}H_{42}N_4O_2$, calculated 1511.3341; found 1510.0508.

2.4 | Synthesis of ZnP-C60 dyad (Scheme 1)

H2P-C60 dyad (6.62μM) was dissolved in 20-mL chloroform, and thereafter, 19.86μM of zinc acetate dihydrate was added to the solution. The reaction mixture was stirred and heated at 60°C for 18 hours resulting in a rosy pink solution. Reaction mixture was washed with water several times, and organic layer was dried over anhydrous sodium sulphate. The solvent was removed on rotary-evaporator, and compound was isolated as violet-coloured crystals. Fourier transform infrared spectroscopy (ν, cm^{-1}): 2917, 2849, 1734, 1573, 1425, 1258, 1012, 794, and 698.^1H NMR (400 MHz, $CDCl_3$, δ) (ppm): 2.52 (2H), 2.9 (2H), 3.05 (2H), 7.4 (3H), 7.5 (2H), 7.9 (9H), 8.1 (8H), 8.4 (2H), and 8.67 (8H); UV-vis ($CHCl_3$, nm): 328, 419, 509, 547, 584, and 752; HR-MS (MALDI-TOF): m/z[M-1] for $C_{115}H_{40}N_4O_2Zn$, calculated 1572.9176; found 1571.9117.

2.5 | Characterization techniques

All chemicals and reagents were purchased from Sigma-Aldrich. Pyrrole was freshly distilled before use. Solvents were purified by distillation before use. Poly(3-hexyl)thiophene was purchased from Sigma-Aldrich. All the products were characterized by FTIR using KBr pallets on Perkin Elmer FTIR Spectrum 2. Fourier transform infrared spectroscopy spectra were collected over a range from 3500 to 500 cm^{-1}. A background in air was done before scanning the samples. Ultraviolet-visible spectroscopy measurement was performed on a Shimadzu UV-vis spectrophotometer (UV-1800) in different polarity solvents. ^1H and ^{13}C NMR spectra were recorded on Jeol 400 MHz spectrometer in $CDCl_3$ using tetramethylsilane as internal standard. Molecular weights of the products were confirmed from MALDI-TOF mass spectrometry on AB SCIEX using α-cyano 4-hydroxy cinnamic acid matrix. Microstructure of materials has been characterized by scanning electron microscope (SEM), EVO MA10, and high-resolution transmission electron microscope analysis on Technai G^2 F30, HV-300.0 kV using. Samples were prepared on glass substrate for SEM analysis by spin-coating dilute solution of dyads in chloroform. Same solution was used for preparation of high-resolution transmission electron microscope sample on 200 mesh copper grids by drop cast. Cyclic voltammetry measurements were performed using a 3-electrode standard configuration with a platinum wire as counter electrode and Ag wire as reference electrode and Pt-disc as working electrode in a 0.1M TBAPF6 (tetra-n-butylammonium hexafluorophosphate) in chlorobenzene solution as electrolyte. Current vs voltage was measured on an Autolab potentiostat. Emission fluorescence measurements were performed on varian (CARY eclipse) fluorescence spectrophotometer in different polarity solvents using 12.5μM solution. Horiba Jobin Yvon (Fluorohub) was used to record time-resolved fluorescence. To perform ultrafast optical pump-probe spectroscopy, we split a train of optical pulse from a Ti:Sapphire laser amplifier (35 fs, 4 mJ/pulse, 1 KHz, 800 nm) into 2 beams with a

beam splitter. One with high intensity was used as a pump, and an optical parametric amplifier (TOPAS, light conversion) was used to vary the wavelength of this pump beam from 190 to 2600 nm. The other beam with weak intensity was propagated through a CaF2 crystal to generate white light continuum covering the whole spectrum of visible light to be used as a probe beam. The probe beam was optically delayed with respect to pump beam using a computer-controlled delay stage. The intrinsic temporal resolution of delay stage is 7 fs. Here, we have performed ultrafast pump-probe spectroscopy using 420 nm as a pump beam at normal incidence, and the changes in absorption was detected by using a gated CMOS detector. The time-resolved study was performed using HELIOS (ultrafast systems) spectrometer.

2.6 | Bulk heterojunction device fabrication

The BHJ OPVs were fabricated with the basic diode configuration of ITO (anode)/PEDOT:PSS (hole transport layer)/Dyad:P3HT (3:1)/Al (cathode). Glass plate coated with transparent ITO electrode and ultrasonically cleaned with detergent, distilled water, acetone, and isopropyl alcohol was dried and used as anode. A thin (10 nm) layer of PEDOT:PSS was spin coated on these glass substrates to act as hole transport layer. Chlorobenzene: chloroform solutions (4:1) of Dyad:P3HT (3:1) (20 mg/mL) were spin coated on top of PEDOT:PSS (~100 nm) while filtering from 0.45 micron PTFE filters in air followed by annealing at 100°C for 20 minutes. Al (100 nm) cathode was deposited on top of active layer under vacuum to yield an area of 6 mm^2 per pixel. The performance of BHJ PSCs were measured using a calibrated AM1.5 solar simulator with a light intensity of 100 mW/cm^2 adjusted using a standard PV reference cell and computer controlled Keithley 236 source measure unit. All fabrication steps and characterizations were performed in ambient without a protective atmosphere.

3 | RESULTS AND DISCUSSION

In this work, we have synthesized simple dyad molecules, ie, H2P-C60 and ZnP-C60, to avoid the complexity in understanding the charge transfer behaviour in porphyrin-fullerene dyad systems to find better candidate for SMOSCs. Several types of covalently linked dyads, triads, tetrads, etc have been synthesized and studied for their photochemical and electrochemical properties where the formation of large well-defined arrays (self-assembly) of such molecules is highly desirable for ordered architectures and efficient light harvesting, charge generation, and separation.[40] Even the simple donor-acceptor systems with perfect geometries and donor-acceptor distances allow efficient electron transfer.[41] In this work, we have also analyzed the packing behaviour of both the dyads by microscopy to find out their self-assembling properties. Several types of synthesis processes are reported for A3B-type porphyrin synthesis, and among all Adler process is the most exploited one to obtain porphyrin in good yield.[42] In this work, porphyrin H2P (Scheme 1) is synthesized by Adler process where the 2 aldehydes, benzaldehyde, and 4-hydroxy benzaldehyde are used in 1:3 molar ratio. Propionic acid is used to act as catalyst for the reaction and also as reaction medium. For the propionic acid solution of 4-hydroxy benzaldehyde, benzaldehyde and freshly distilled pyrrole are added simultaneously drop wise. Reaction mixture is refluxed for approximately 30 minutes while protecting from sunlight. On neutralization of reaction mixture with saturated sodium bicarbonate solution, the crude material precipitates out. Column chromatography is used to isolate the desired A3B porphyrin (H2P) that comes as second band after meso-tetraphenylpophyrin in dichloromethane. Porphyrin H2P is formed in good yield (~12% on average) via this process. On the other hand, fullerene acceptor part is prepared by hydrolyzing PC61BM synthesized by our reported process.[43] Phenyl-C61-butyric acid methyl ester is hydrolyzed in acidic medium to form PCBA. H2P and PCBA are linked together by Steglich esterification reaction in the presence of N,N′-dicyclohexylcarbodiimide and 4-dimethylaminopyridine. Product H2P-C60 dyad is collected by column chromatography using toluene as eluent. For synthesis of metallated dyad ZnP-C60, reaction of H2P-C60 with zinc acetate dihydrate is performed in chloroform. All the products are characterized by different spectroscopic techniques for the establishment of their structure (see Section 2 for details), and electron microscopic studies have been performed to ascertain their self-assembling properties. In looking at the SEM and TEM images of H2P-C60 and ZnP-C60 dyads (Figure 1), we can see a clear difference in self-assembling behaviour of the 2 dyads. The nonmetallated dyad, H2P-C60, forms more fibrous structure while metallated dyad, ZnP-C60, remains as globules. TEM image of H2P-C60 shows the formation of layer by layer stacked self-assembly with a separation of approximately 2 nm in height while no such behaviour is seen for ZnP-C60 dyad.[44] We further analyzed the dyads for ground state and excited state interaction between donor and acceptor components by different techniques as discussed below.

4 | GROUND STATE INTERACTION STUDY

4.1 | Electrochemical analysis and electron transfer driving force

The cyclic voltammetry was performed in dry chlorobenzene and using 0.1M supporting electrolyte (n-Bu_4NPF_6). Three electrode systems were used with a platinum disc as working electrode and a silver wire and a platinum wire as reference and counter electrodes, respectively. Ferrocene/ferricenium couple was an internal reference to calibrate the redox

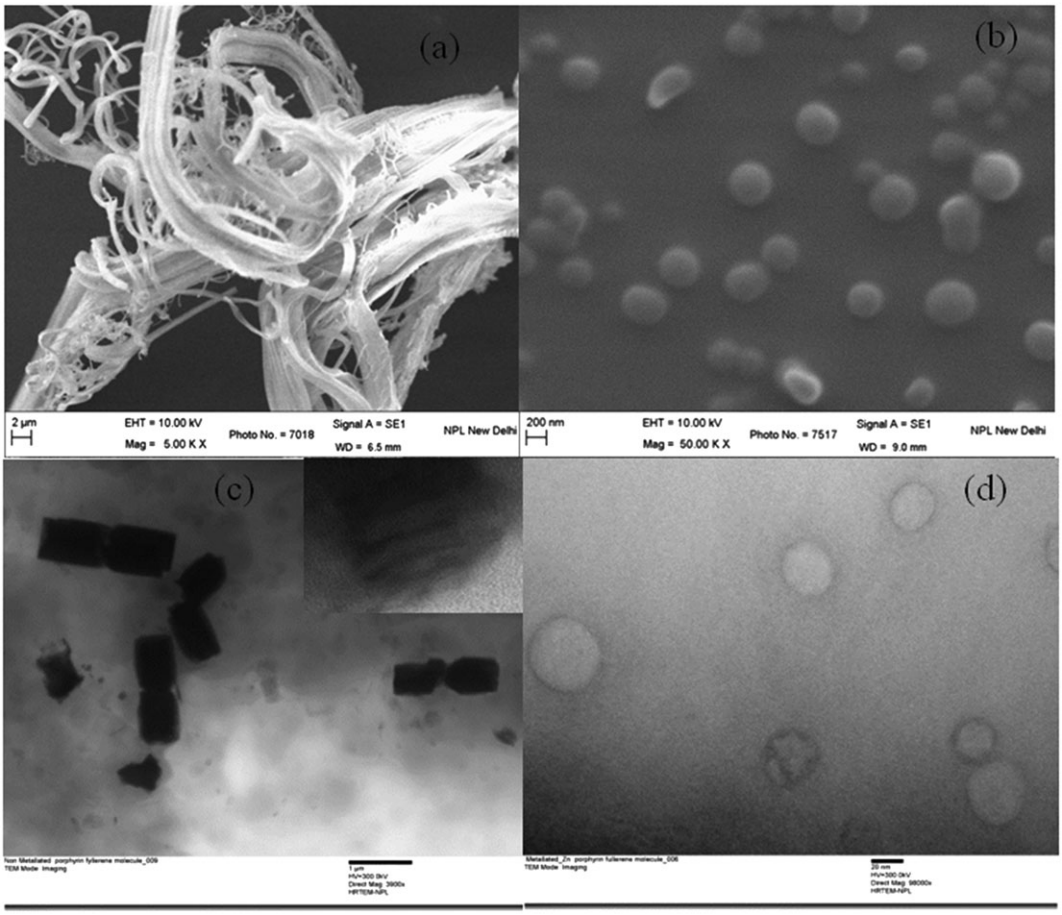

FIGURE 1 Scanning electron microscope images of, A, H2P-C60 and, B, ZnP-C60 and TEM images of, C, H2P-C60 and, D, ZnP-C60

potentials. The redox potentials of H2P, H2P-C60, and ZnP-C60 are summarized in Table 1.

Nonmetallated dyad H2P-C60 shows 1 reversible oxidation and 5 reversible reduction potentials in chlorobenzene (Figure 2D). While metallated dyad ZnP-C60 shows 2 reversible oxidation potentials at 0.40 and 0.63 V for metal and porphyrin ring oxidation, respectively (Figure 2E). ZnP-C60 shows higher potential for porphyrin ring oxidation compared with H2P-C60, suggesting easier oxidation of porphyrin ring in nonmetallated system that will help in fast charge generation and separation. ZnP-C60 dyad also shows 5 reversible reduction potential akin to H2P-C60 but at higher voltages.With the help of electrochemical data, the driving force ($-\Delta G^{o}_{ET}$) for intramolecular electron transfer process was calculated for dyads (Table 1).[45] The driving forces ($-\Delta G^{o}_{ET(CR)}$ in eV) for intramolecular charge recombination processes from C60 radical anion ($C60^{-}$) to porphyrin radical cation ($H2^{\cdot+}$) or $C60^{-}$ to $ZnP^{+}$are calculated by Weller Equation 1,[46] where *e* stands for elementary charge,

$$-\Delta G^{o}_{ET(CR)} = e\left[E^{o}_{ox}\left(\frac{D^{\cdot+}}{D}\right) - E^{o}_{red}\left(\frac{A}{A^{-}}\right)\right] \ldots\ldots\ldots \quad (1)$$

$E^{o}_{ox}(D^{+}/D)$ is the first oxidation potential of donor (H2P or ZnP) moiety while $E^{o}_{red}(A/A^{-})$ refers to first reduction potential of acceptor (C_{60}) moiety in chloroform, chlorobenzene, and THF. Furthermore, the driving force ($-\Delta G^{o}_{ET(CR)}$ in eV) for intramolecular charge separation process was determined by following Equation 2:

$$-\Delta G^{o}_{ET(CS)} = \Delta E_{0\text{–}0} + \Delta G^{o}_{(CR)} \ldots\ldots\ldots\ldots \quad (2)$$

where the $\Delta E_{o\text{-}o}$ is the energy of the o-o transition energy gap between lowest singlet excited state and the ground state.

TABLE 1 Redox potentials (E^{o}) of H2P, dyad H2P-C60, and ZnP-C60 in various solvents (v/sFc/Fc^{+})

	Chlorobenzene (ε = 5.62)		$-\Delta G^{o}_{ET}$ (eV) CR CS Chlorobenzene	
	E^{o}_{ox}/V	E^{o}_{red}/V		
H2P	0.54	−0.85 −1.92 −2.26	1.39	0.50
H2P-C60	0.55	−1.21 −1.58 −1.80 −1.94 −2.11	1.76	0.10
ZnP-C60	0.40 0.63	−1.27 −1.60 −2.02 −2.19 −2.37	1.67	0.19

The redox potentials were measured by cyclic voltammetry in chlorobenzene with 0.1M n-Bu_4NPF_6 as a supporting electrolyte with a scan rate of 10 mV s^{-1}. $-\Delta G^{o}_{ET(CR)}$ and $-\Delta G^{o}_{ET(CS)}$ are the driving force for intramolecular electron transfer for charge recombination and charge separation processes, respectively, calculated by Equations 1 and 2.

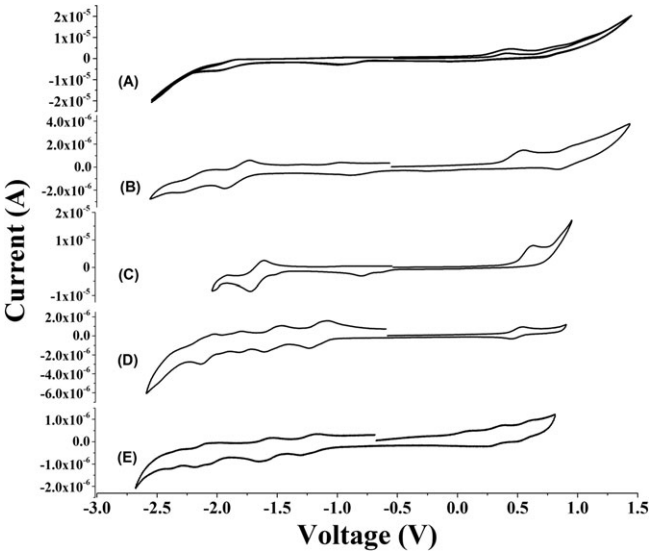

FIGURE 2 Cyclic voltammograms of, A, H2P, B, H2P-C60, and, C, ZnP-C60 in chlorobenzene (v/s Fc/Fc^{+}) with 0.1M n-Bu_4NPF_6 as a supporting electrolyte with a scan rate of 10 mV s^{-1}

Base-free porphyrin dyad (H2P-C60) shows much lower driving force for charge separation and higher for charge recombination (0.10 eV and 1.76 eV, respectively) compared with ZnP-C60 dyad (0.19 eV and 1.67 eV, respectively) resulting in more efficient and long-lived charge separated state in base-free porphyrin dyads.

4.2 | Steady-state absorption spectroscopy

Ground state absorption spectra of porphyrin shows several absorption bands corresponding to transition to first or higher singlet excited states.[47] Two or more weak transitions occur in 500 to 600 nm region corresponding to S_0-S_1 transition, ie, first singlet excited state from ground state. These transitions are quasi allowed and hence called Q-bands. Another allowed transition to second singlet excited state (S_2) appears very strong in the range of 400 to 420 nm and known as Soret band (or B-band). Ultraviolet-visible absorption spectra of H2P-C60 and ZnP-C60 dyads were recorded in chloroform for qualitative analysis and compared with H2P and PC61BM as shown in Figure 3. H2P porphyrin shows strong Soret band at 412 nm followed by Q-bands at 515, 550, 591, and 650 nm. H2P-C60 dyad features absorption maxima at 328 (fullerene absorption), 418 (Soret band), 508, 549, 590, and 650 nm (Q-bands). ZnP-C60 dyad shows absorption maxima at 328 (fullerene absorption), 419 (Soret band), 509, 547, 584, and 752 nm (very low-intensity Q-bands). Additional absorption band at 330 nm in dyads confirms the formation of fullerene-linked porphyrin dyad system (Figure 3). However, absorption band at 430 nm for monofunctionalized fullerene derivatives could not be seen here because of overlapping with strong porphyrin Soret band absorption. The absorption spectra of dyads shows slight red shift in Soret bands (~6 nm). An absorption at approximately 900 nm (inset Figure 3) in dyads for charge transfer band also ascertains the effective charge transfer between porphyrin donor and fullerene acceptor in dyads in ground state.

To further understand the absorption behaviour of dyads, we perform absorption study in different polarity solvents and compared with H2P porphyrin reference for same concentration (12.5μM) in hexane, toluene, DCM, dichloroethylene (DCE), chloroform, ethyl acetate, dimethyl formamide, and dimethyl sulfoxide with increasing polarity (0.0 to 7.2) (Figure 4). Peak positions and absorption coefficients are summarized in Table S1. Dyads show decreased absorption coefficient compared with porphyrin precursor

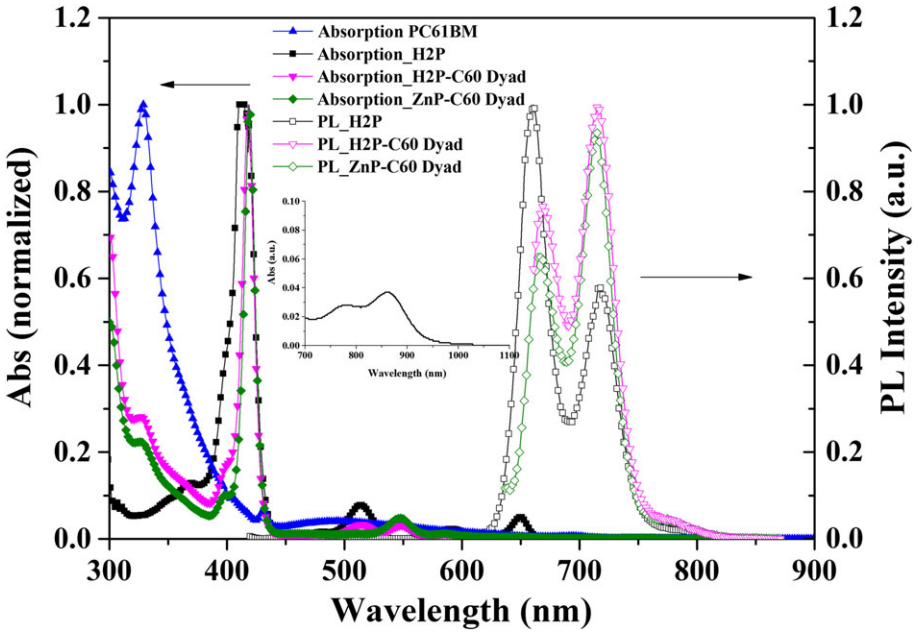

FIGURE 3 Normalized ultraviolet absorption and photoluminescence emission spectra of H2P, H2P-C60, and ZnP-C60 in chloroform. Inset shows charge transfer band in dyads. Absorption spectra of phenyl-C61-butyric acid methyl ester (PC61BM) are also shown for comparison

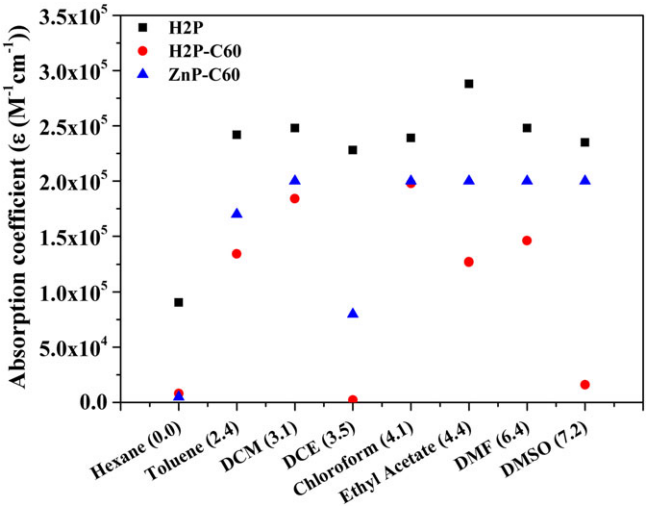

FIGURE 4 Change in absorption coefficient for Soret band with change in solvent polarity for 12.5μM solution of H2P, H2P-C60, and ZnP-C60. DCE indicates dichloroethylene

because of ground state intramolecular interactions. The maximum absorption of Soret band in porphyrin was obtained in ethyl acetate while dyads show maximum absorption in chlorinated solvents (dichloromethane and chloroform). Completely different absorption behaviours were observed in dichloroethylene. Highly red shifted Soret band was recorded in nonmetallated H2P-C60 and porphyrin reference H2P. Such behaviour was not detected in ZnP-C60, suggesting a strong interaction between unsaturated solvent and nonmetallated porphyrin core. ZnP-C60 shows stronger absorbance for all the solvents compared with H2P-C60 dyad except DCE. Red shifted bands are observed in ZnP-C60 on increasing polarity while no significant shift is noticed in case of H2P-C60 dyad. Shifts in absorption bands along with change in absorption coefficient compared with porphyrin suggest significant ground state electronic interaction in dyad materials. Also, the low-absorption intensity suggests the formation of aggregation for dyads in nonpolar solvent (hexane) and highly polar solvent (DMSO).

5 | EXCITED STATE INTERACTION STUDY

5.1 | Steady-state fluorescence

Steady-state fluorescence from S1 state, ie, S1[0] to S0[0] (transition 1) and S1[0] to S0[1] (transition 2) in porphyrin H2P, is observed at 660 and 718 nm on excitation with Soret band wavelength (Figures 3 and 5). Similarly for H2P-C60 and ZnP-C60 dyads, the emission bands appear at 670 and 716 nm and 667 and 714 nm, respectively (Figure 3). H2P-C60 shows approximately 7 to 10 nm red shift for transition 1 compared with porphyrin precursor while ZnP-C60 dyad shows appreciable shift compared with precursor porphyrin because of intramolecular electron transfer between donor and acceptor components on excitation in dyads. Figure 5 shows the comparative fluorescence spectra for 12.5μM solutions of H2P, H2P-C60, and ZnP-C60 dyads (same solutions used in absorption measurement) in toluene, dichloromethane, DCE, chloroform, ethyl acetate, dimethylformamide, and dimethyl sulfoxide. Intensity of emission for H2P increases with increase in solvent polarity; however, fluorescence intensity is quenched more efficiently in dyads with increasing solvent polarity because of more efficient charge transfer from donor to acceptor and better solvation for charged species. Transition 1 shows an increase in intensity on increasing polarity of solvents similar to reference porphyrin H2P in both the dyads while intensity of transition 2 quenches with solvent polarity (Figure 5).

While in H2P-C60, transition 1 red shifts on varying solvent polarity from toluene (2.4) to ethyl acetate (4.4) and again highly blue shift in DMF (6.4) and DMSO (7.2). Transition 2 remains in the same position except in ethyl acetate where it is red shifted by approximately 6 nm. In contrast to H2P-C60, in ZnP-C60, no significant shift is observed in transition 1 on varying solvent polarity from toluene (2.4) to ethyl acetate (4.4) while it red shifts in DMF (6.4) and DMSO (7.2). Red shifts of 4, 10, and 12 nm are observed for transition 2 in ethyl acetate, DMF, and DMSO, respectively, compared with toluene in ZnP-C60. Thus, significantly different photoluminescence behaviours are shown by the 2 types of dyads. The emission peak of fullerene[48] is highly quenched in both the dyads in all the solvents suggesting very weak energy transfer from singlet excited porphyrin unit to fullerene on excitation.

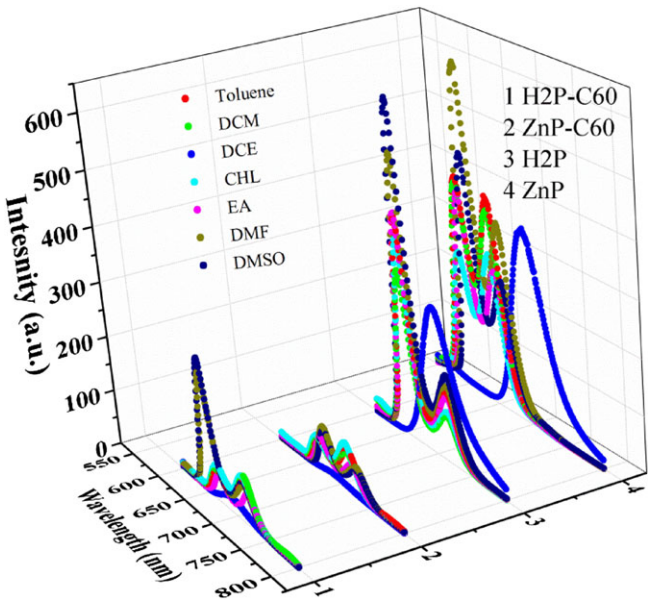

FIGURE 5 Plot of fluorescence spectra in different polarity solvents for equimolar solutions of, A, H2P-C60, B, ZnP-C60, C, H2P, and, D, ZnP. CHL indicates chloroform; DCE, dichloroethylene; EA, ethyl acetate

TABLE 2 Time-resolved fluorescence data recorded in different polarity solvents for 12.5μM solutions of H2P, H2P-C60, ZnP, and ZnP-C60

	H2P		$H2P^{*1}$-C60			
	λ_{em}, nm	τ, ns	λ_{em}, nm	τ, ns	$k_{ET(CS)}$, s^{-1}	ϕ_{CS}
Toluene	654	8.2	668	2.2	0.33×10^9	0.73
DCM	653	7.3	667	2.8	0.21×10^9	0.60
DCE	704	2.3	693	0.63	1.1×10^9	0.71
CHL	655	6.6	670	2.2	0.3×10^9	0.67
EA	653	8.2	671	2.0	0.38×10^9	0.76
DMF	654	9.8	652	1.7	0.49×10^9	0.83
DMSO	654	10.1	651	0.19	5.1×10^9	0.98
	ZnP		ZnP^{*1}-C60			
	λ_{em}, nm	τ, ns	λ_{em}, nm	τ, ns	$k_{ET(CS)}$, s^{-1}	ϕ_{CS}
Toluene	600	3.0	669	0.82	1.1×10^9	0.90
DCM	600	3.1	668	0.93	0.93×10^9	0.87
DCE	700	2.3	692	1.5	0.23×10^9	0.35
CHL	598	3.4	667	1.2	0.1×10^9	0.40
EA	602	2.8	671	2.2	0.33×10^9	0.73
DMF	608	2.5	676	2.2	0.35×10^9	0.77
DMSO	610	1.7	678	1.0	0.9×10^9	0.89

Abbreviation: CHL indicates chloroform; DCE, dichloroethylene; EA, ethyl acetate.

Time-resolved fluorescence data recorded in different polarity solvents for transitions 1 and 2. τ is the lifetime of singlet excited states in nanosecond; $k_{ET(CS)}$ is rate of charge separation per second; ϕ_{CS} is efficiency of charge separation.

5.2 | Dependence of lifetime on solvent polarity

We also calculated the singlet excited state lifetimes (τ) of dyads and porphyrin H2P with a time-correlated single photon counting apparatus by using 460-nm excitation in different polarity solvents for equimolar concentrations (Table 2 and Figure 6). The fluorescence decay was monitored at transition 1 for porphyrin, H2P-C60, and ZnP-C60 dyads for 12.5μM concentration in hexane, toluene, DCM, DCE, chloroform, ethyl acetate, dimethyl formamide, and dimethyl sulfoxide with increasing polarity. The fluorescence decay curves were well fitted by monoexponential decay component. Lifetime of singlet excited states is highly decreased in dyads compared with porphyrin precursor H2P and ZnP because of charge transfer from porphyrin-excited state to fullerene moiety for the formation of charge-separated states.On the basis of fluorescence lifetimes for porphyrin and dyads in different polarity solvents, electron transfer rate constant for charge separation ($k_{ET(CS)}$) was calculated using following Equation 3, and the efficiency (ϕ_{CS}) was calculated from Equation 4 for $H2P^{+}$-$C60^{-}$ formation.

$$k_{ET(CS)} = \frac{1}{\tau(\text{dyad})} - \frac{1}{\tau(\text{porphyrin})} \ldots \quad (3)$$

$$\phi_{(CS)}\left(H2P^{*1}\right) = \frac{\frac{1}{\tau(\text{dyad})} - \frac{1}{\tau(\text{porphyrin})}}{\frac{1}{\tau(\text{dyad})}} \ldots\ldots \quad (4)$$

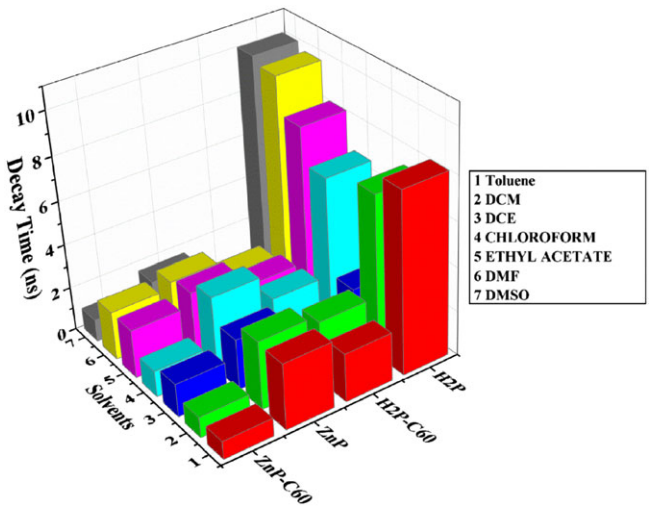

FIGURE 6 Bar diagram showing singlet excited state lifetime (τ) of H2P, H2P-C60, ZnP, and ZnP-C60 in different polarity solvents for transition 1. DCE indicates dichloroethylene

Lifetime of singlet excited state of porphyrin $H2P^{*1}$ or ZnP^{*1} shows different behaviours on increasing solvent polarity. $H2P^{*1}$ species is long lived in less polar solvents, ie, toluene and DCM, whereas ZnP^{*1} decays rapidly in these solvents. On the other hand, $H2P^{*1}$ species is short lived and decays into charge-separated states ultrafast in polar solvents. Shortest lifetime of $H2P^{*1}$ and ZnP^{*1} was recorded in DMSO and toluene, respectively. Efficiency of charge separation (ϕ_{CS}) is greater than 60% in all the solvents for H2P-C60 dyad and approximately 98% in DMSO that means maximum $H2P^{*1}$ state is converting into charge-separated state. On the other hand, ZnP-C60 dyad shows ϕ_{CS} as low as 35% and highest approximately 90% charge separation efficiency is obtained in toluene, DCM, and DMSO that is comparatively very low to H2P-C60 dyad.

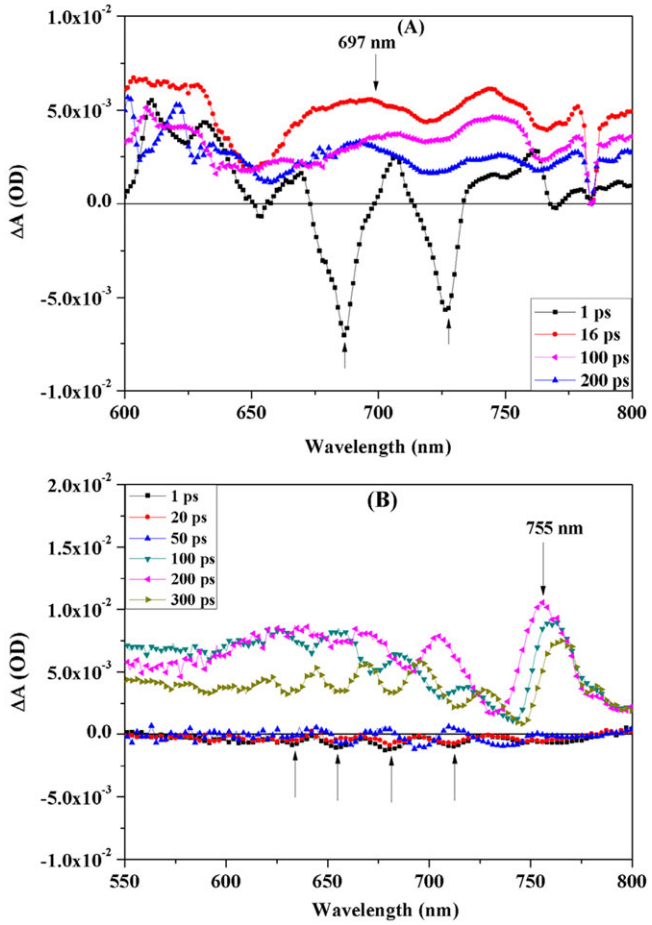

FIGURE 7 Transient absorption spectra for, A, H2P-C60 and, B, ZnP-C60 dyads in chloroform. Upward arrows show the absorption and emission bleaching and downward arrows show transient porphyrin radical cation

5.3 | Transient absorption spectroscopy study

Ultrafast TA spectra of H2P, H2P-C60, and ZnP-C60 dyads were measured by femto and pico second pump-probe analysis in chloroform to evidence the occurrence of photoinduced charge separation from singlet excited state of H2P and ZnP in both the dyads. The recorded transient absorption spectra for H2P-C60 and ZnP-C60 dyads are shown in Figure 7. Transient absorption spectra recorded in solution give direct information regarding the excited states involved and also specify the spectral regions for further electron transport process. Transient absorption spectra gives the information about ground state absorption and singlet excited state emission bleaching, singlet excited state absorption, and triplet excited state absorptions. In this study, we have recorded the TA spectra of porphyrin precursor (H2P) (Table S1), porphyrin-fullerene dyad (H2P-C60), and metalloporphyrin dyad (ZnP-C60) in chloroform solution at several delay times after excitation with 530 nm wavelength.

Immediately after the pump, porphyrin as well as dyads shows bleaching for porphyrin Q-bands at 571, 595, and 650 nm (Figure 7A). In H2P-C60 dyad, singlet excited state absorption and stimulated emission bleaching for $H2P^{*1}$ singlet excited state appeared at 610 and 630 nm and 686 and 727 nm, respectively, within 1 to 2 ps. After 16-ps delay time, new broad transition band appears in H2P-C60 dyad at 697 nm ascribed to $H2P^{+}$ radical cation[49] evolving from photoinduced electron transfer from $H2P^{*1}$ donor to C_{60} acceptor forming $H2P^{+}$ and C_{60}^{-}radicals.

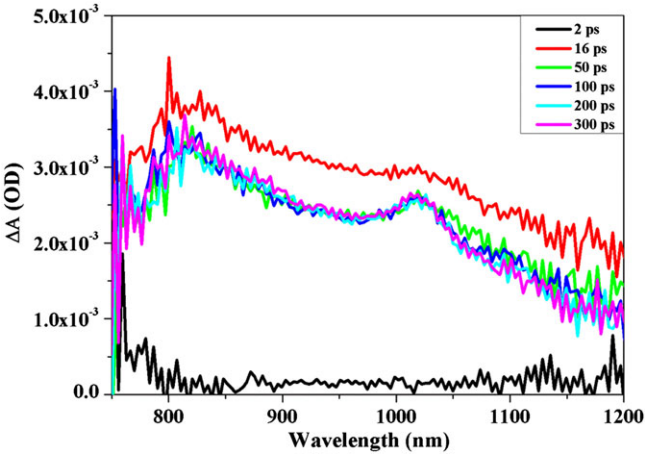

FIGURE 8 Transient absorption spectra in NIR region for H2P-C60 dyad

Simultaneously after 16 ps, transient absorption of C_{60}^{-} radical anion appears at approximately[50] 1045 nm (Figure 8) and $H2P^{*3}$ broad absorption at 845 nm.[51] In case of metallated ZnP-C60 dyad, visible range spectra only shows absorption and emission bleaching at 630, 663, 684, and 727 nm, and the transient species generates comparatively slowly after 100 ps (Figure 7B). We can clearly see ZnP^{+} specie at 755 nm. The transient for ZnP^{*3} appears at 830 nm after 50 ps of excitation. Similarly after 50 ps, transient absorption of C_{60}^{-} radical anion appears at approximately 1035 nm in ZnP-C60 dyad (Figure 9).[48,49] As the decay lasted beyond the monitoring time of our femtosecond transient spectrometer, the lifetime of cation and anion radicals for both the dyads could not be calculated and requires nanosecond transient measurements.

Finally, we tested the materials in single material organic photovoltaic devices using P3HT as matrix. The fabricated

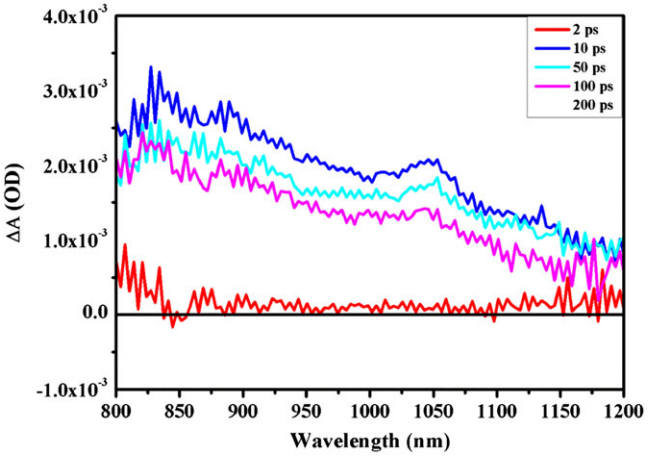

FIGURE 9 Transient absorption spectra in NIR region for ZnP-C60 dyad

OPV device consisted of ITO (anode)/PEDOT:PSS (hole transport layer)/Dyad:P3HT (3:1)/Al (cathode). Device with ZnP-C60 did not show any light effect while the device made H2P-C60 dyad (nonencapsulated and unoptimized) showed promising photovoltaic property. From OPV device J-V characteristics, we calculated the open circuit voltage (V_{oc}) approximately 0.49 V, short circuit current (J_{sc}) of approximately 50 μA/cm^2, and high-fill factor of 0.57 that are much higher than the recently reported device for quinoline-fluorene-based system and previous reports (see ESI).[52,53] Thus, the device data prove the concept of nonmetallated porphyrin-fullerene dyad to be a better candidate in organic solar cell compared with metallated dyads.

6 | CONCLUSION

In conclusion, we have extensively studied a very simple system of covalently bound donor-acceptor dyad and compared the photophysical properties between nonmetallated (H2P-C60) and metallated porphyrin-fullerene (ZnP-C60) dyads to ascertain the better candidate to be used in single material organic solar cell. H2P-C60 shows much better properties than ZnP-C60 for faster oxidation of porphyrin ring at lower voltage for the formation of charged species, high efficiency of charge separation in variety of solvents, and formation of long-lived charge-separated state. H2P-C60 also forms stable and defined self-assembly that is one of the essential criterion for efficient light harvesting, charge generation, and charge separation. Further study of optimization of parameters for SMOSCs is undergoing.

ACKNOWLEDGEMENTS

Authors acknowledge DST (SB/FT/CS-038/2014) and CSIR-TAPSUN for funding, and NG thanks CSIR for fellowship.

REFERENCES

[1] C. J. Brabec, N. S. Sariciftici, J. C. Hummelen, *Adv. Funct. Mater.* **2001**, *11*, 15.

[2] G. Dennler, M. C. Scharber, C. J. Brabec, *Adv. Mater.* **2009**, *21*, 1323.

[3] J. L. Delgado, P. A. Bouit, S. Filippone, M. A. Herranz, N. Martin, *Chem Commun* **2010**, *46*, 4853.

[4] S. Gunes, H. Neugebauer, N. S. Sariciftci, *Chem. Rev.* **2007**, *107*, 1324.

[5] A. Opitz, J. Wagner, W. Brütting, I. Salzmann, N. Koch, J. Manara, J. Pflaum, A. Hinderhofer, F. Schreiber, *Quantum Electron.* **2010**, *16*, 1707.

[6] B. Ray, A. G. Baradwaj, M. R. Khan, B. W. Boudouris, M. A. Alam, *PNAS* **2015**, *112*, 11193.

[7] V. C. Kumar, L. Cabau, E. N. Koukaras, G. D. Sharma, E. Palomares, *Nanoscale* **2015**, *7*, 179.

[8] M. K. Panda, K. Ladomenou, A. G. Coutsolelos, *Coord. Chem. Rev.* **2012**, *256*, 2601.

[9] M. G. Walter, A. B. Rudine, C. C. Wamser, *J. Porphyrins Phthalocyanines* **2010**, *14*, 759.

[10] A. Thompson, T. S. Ahn, K. R. Justin, T. S. Thayumanavan, T. J. Martínez, C. J. Bardeen, *J. Am. Chem. Soc.* **2005**, *127*, 16348.

[11] A. S. Konev, A. F. Khlebnikov, T. G. Nikiforova, A. A. Virtsev, H. Frauendorf, *J Org Chem* **2013**, *78*, 2542.

[12] L.-C. Song, X.-F. Liu, Z.-J. Xie, F.-X. Luo, H.-B. Song, *Inorg. Chem.* **2011**, *50*, 11162.

[13] X. Cao, W. Lin, Q. Yu, *J Org Chem* **2011**, *76*, 7423.

[14] A. Ellis, D. Gooch, L. J. Twyman, *J Org Chem* **2013**, *78*, 5364.

[15] J.-K. Rhee, M. Baksh, C. Nycholat, J. C. Paulson, H. Kitagishi, M. G. Finn, *Biomacromolecules* **2012**, *13*, 2333.

[16] P. A. Liddell, D. Kuciauskas, J. P. Sumida, B. Nash, D. Nguyen, A. L. Moore, T. A. Moore, D. Gust, *J. Am. Chem. Soc.* **1997**, *119*, 1400.

[17] G. Kodis, P. A. Liddell, A. L. Moore, T. A. Moore, D. Gust, *J. Phys. Org. Chem.* **2004**, *17*, 724.

[18] D. Gust, T. A. Moore, A. L. Moore, *Acc. Chem. Res.* **2001**, *34*, 40.

[19] M. E. El-Khouly, O. Ito, P. M. Smith, F. D'Souza, *J Photochem Photobiol C* **2004**, *5*, 79.

[20] R. C. Haddon, L. E. Brus, K. Raghavachari, *Chem. Phys. Lett.* **1986**, *125*, 459.

[21] S. Kirner, M. Sekita, D. M. Guldi, *Adv. Mater.* **2014**, *26*, 1482.

[22] A. D. J. Haymet, *Chem. Phys. Lett.* **1985**, *122*, 421.

[23] D. M. Guldi, *Pure Appl. Chem.* **2003**, *75*, 1069.

[24] D. M. Guldi, M. Prato, *Chem Commun* **2004**, *22*, 2517.

[25] M. H. Lee, B. D. Dunietz, E. Geva, *J. Phys. Chem. C* **2013**, *117*, 23391.

[26] A. K. Manna, B. D. Dunietz, *J Chem Phys* **2014**, *141*, 121102-(1).

[27] M. Wang, F. Wudl, *J. Mater. Chem.* **2012**, *22*, 24297.

[28] S. Fukuzumi, K. Ohkuboa, *DaltonTrans* **2013**, *42*, 15846.

[29] M. P. Eng, B. Albinsson, *Angew Chem Int Ed* **2006**, *45*, 5626.

[30] S. V. Kirner, D. Arteaga, C. Henkel, J. T. Margraf, N. Alegret, B. K. Ohkubo, A. Ortiz, N. Martin, L. Echegoyen, S. Fukuzumi, T. Clark, D. M. Guldi, *Chem Sc* **2015**, *6*, 5994.

[31] F. Giacalone, J. L. Segura, N. Martin, D. M. Guldi, *J. Am. Chem. Soc.* **2004**, *126*, 5340. M. R. Wasielewski, W. B. Davis, W. A. Svec, M. A. Ratner, *Nature* **1998**, *396*, 60. B. Albinsson, M. P. Eng, K. Pettersson, M. U. Winters, *Phys. Chem. Chem. Phys.* **2007**, *9*, 5847.

[32] A. F. Mironov, *Macroheterocycles* **2011**, *4*, 186.

[33] G. D. Torre, F. Giacalone, J. L. Segura, N. Martin, D. M. Guldi, *Chem. – Eur. J.* **2005**, *11*, 1267.

[34] A. M. Ontoria, M. Wielopolski, J. Gebhardt, A. Gouloumis, T. Clark, D. M. Guldi, N. Martin, *J. Am. Chem. Soc.* **2011**, *133*, 2370.

[35] M. Wielopolski, A. M. Ontoria, C. Schubert, J. T. Margraf, E. Krokos, J. Kirschner, A. Gouloumis, T. Clark, D. M. Guldi, N. Martin, *J. Am. Chem. Soc.* **2013**, *135*, 10372.

[36] S. Wolfrum, J. R. Pinzon, A. M. Ontoria, A. Gouloumis, N. Martin, L. Echegoyen, D. M. Guldi, *Chem.Commun.* **2011**, *47*, 2270.

[37] F. Oswald, D. M. Islam, Y. Araki, V. Troiani, R. Caballero, P. de la Cruz, O. Ito, F. Langa, *ChemCommun* **2007**, *43*, 4498.

[38] F. Oswald, D. M. Islam, M. E. El-Khouly, Y. Araki, R. Caballero, P. de la Cruz, O. Ito, F. Langa, *Phys. Chem. Chem. Phys.* **2014**, *16*, 2443.

[39] D. Kuciauskas, P. A. Liddell, S. Lin, S. G. Stone, A. L. Moore, T. A. Moore, D. Gust, *J Phys Chem B* **2000**, *104*, 4307.

[40] M. R. Wasielewski, *Acc. Chem. Res.* **2009**, *42*, 1910.

[41] C. Schubert, J. T. Margraf, T. Clark, D. M. Guldi, *Chem. Soc. Rev.* **2015**, *44*, 988.

[42] A. D. Adler, F. R. Longo, J. D. Finarelli, J. Goldmacher, J. Assour, L. Korsakoff, *J Org Chem* **1967**, *32*, 476.

[43] R. Kumar, S. Naqvi, N. Gupta, S. Chand, *RSC Adv.* **2014**, *4*, 15675.

[44] C.-L. Wang, W.-B. Zhang, R. M. Van Horn, Y. Tu, X. Gong, S. Z. D. Cheng, Y. Sun, M. Tong, J. Seo, B. B. Y. Hsu, A. H. Heeger, *Adv. Mater.* **2011**, *23*, 2951.

[45] R. A. Marcus, *J Chem Phys* **1956**, *24*, 966.

[46] Z. A. Weller, *Phys Chem NeueFolge* **1982**, *133*, 93.

[47] M. Gouterman, *J Mol Spectroscopy* **1961**, *6*, 138.

[48] D. Kuciauskas, S. Lin, G. R. Seely, A. L. Moore, T. A. Moore, D. Gust, T. Drovetskaya, C. A. Reed, P. D. W. Boyd, *J Phys Chem* **1996**, *100*, 15926.

[49] S. V. Kirner, D. M. Guldi, J. D. Megiatto, D. I. Schuster, *Nanoscale* **2015**, *7*, 1145.

[50] D. M. Guldi, M. Prato, *Acc. Chem. Res.* **2000**, *33*, 695.

[51] O. Ito, *Res Chem lntermed* **1997**, *23*, 389.

[52] A. Slodek, M. Matussek, M. Filapek, G. Szafraniec-Gorol, A. Szlapa, I. Grudzka-Flak, M. Szczurek, J. G. Malecki, A. Maron, E. Schab-Balcerzak, E. M. Nowak, J. Sanetra, M. Olejnik, W. Danikiewicz, S. Krompiec, A. Slodek, *Eur. J. Org. Chem.* **2016**, *14*, 2500.

[53] G. Possamai, S. Marcuz, M. Maggini, E. Menna, L. Franco, M. Ruzzi, S. Ceola, C. Corvaja, G. Ridolfi, A. Geri, N. Camaioni, D. M. Guldi, R. Sens, T. Gessner, *Chem. – Eur. J.* **2005**, *11*, 5765.

SUPPORTING INFORMATION

Additional Supporting Information may be found online in the supporting information tab for this article.

How to cite this article: Gupta N, Naqvi S, Jewariya M, Chand S, Kumar R. Comparative charge transfer studies in nonmetallated and metallated porphyrin fullerene dyads. *J Phys Org Chem*. 2017;e3685. https://doi.org/10.1002/poc.3685